Available at: http://publications.ictp.it IC/2009/093

United Nations Educational, Scientific and Cultural Organization
and
International Atomic Energy Agency

THE ABDUS SALAM INTERNATIONAL CENTRE FOR THEORETICAL PHYSICS

SIMULATION OF SYNOPTIC SCALE CIRCULATION FEATURES OVER SOUTHERN AFRICA USING GCMS

Nana Ama Kum Browne[1]
Climate Systems Analysis Group, Environmental and Geographical Science, University of Cape Town, South Africa,
Department of Physics, University of Cape Coast, Cape Coast, Ghana
and
The Abdus Salam International Centre for Theoretical Physics, Trieste, Italy,

Babatunde Joseph Abiodun, Mark Tadross and Bruce Hewitson
Climate Systems Analysis Group, Environmental and Geographical Science, University of Cape Town, South Africa.

Abstract

Two global models (HadAM3: The Hadley Centre Atmospheric Model version 3 and CAM3: The Community Atmospheric model version 3) have been studied regarding their capabilities in reproducing the small scale features over southern Africa compared with the NCEP reanalysis. In this study, geopotential height at 500hPa and 850hPa pressure levels are used to investigate the variability of small scale circulation features over southern Africa. The investigation took into consideration the magnitude of the models standard deviations. Most of the results were linked with rainfall and temperature over the region. It was found that the standardized anomalies in the geopotential height at the 500hPa pressure level are in phase with that of rainfall. In contrast, the standardized anomalies of 850hPa pressure level geopotential height are out of phase with the standardized anomalies of rainfall and temperature. In addition, the models are able to capture the variation in the mean cut-off lows, number of days with deep tropical lows and number of days with Tropical Temperate Troughs (TTTs) quite well. However, the models could not capture the number of days with temperate lows very well. Generally, the models are able to reproduce the synoptic scale circulation features which are crucial for reliable seasonal forecast over southern Africa.

MIRAMARE — TRIESTE

November 2009

[1] Junior Associate of ICTP. Corresponding author: nbrowne@csag.uct.ac.za

1. Introduction

Seasonal variability in the southern African climate strongly depends on synoptic scale circulation systems (Tyson, 1981; Tyson and Preston-Whyte, 2000). The synoptic scale features considered here are small scale features such as cut-off lows, deep tropical lows, deep temperate lows and Tropical Temperate Troughs (TTTs). These features are very transient and short lived. However, they interact with the large scale circulation and their interactions determine the southern African climate (Hudson and Jones, 2002; Reason and Jagadheesha, 2005; Anyah and Semazzi, 2006). In many cases, when the small features interact with the large scale circulation, they produce intense weather conditions. Additionally, their interactions significantly affect the Sea Surface Temperature (SST) (Qiu et al. 2004), which is normally used to force seasonal forecasting. Seasonal rainfall over southern Africa is a result of the interaction of different small scale and large scale circulation systems over the region. However, it is difficult to predict the rainfall distribution caused by the small scale features because the complex terrain of the region may enhance or inhibit convective activities of the synoptic features (Nieto et al. 2007; Hobbs et al. 1998). Therefore, investigating the possible variations of the small scale features is very important and topical in seasonal forecasting.

The predominant small scale features in southern African climate that induce rainfall may include cut-off lows, deep tropical lows, deep temperate lows and tropical temperate troughs (Hobbs et al. 1998; Harrison 1984a; 1984b; Todd and Washington, 1999; Tyson and Preston-Whyte 2000; Jury and Nkosi 2000). These waves are well recognized at 500hPa height and are deep if they extend near the surface at 850hPa. Disturbances in the mid-latitude westerlies include the troughs, cold fronts and cut-off lows. The frequency, duration and intensity of these circulation features either induce or suppress rainfall, thus leading to rainfall variability over southern Africa (Harrison 1984; Tyson and Preston-Whyte 2000). For example, Taljaard (1985) showed that the westerly disturbances and the formation of cut-off lows induce rainfall. Cut-off lows seen in the upper air as a trough, deepens until it forms a closed circulation. This deep closed circulation that develops from an upper westerly trough is one of the most intense synoptic features over southern Africa. It induces unstable troposphere at low levels, produces severe convective events that lead to heavy rainfall and floods over large areas, and may trigger severe cyclonegenesis that induces strong wind (Nieto et al 2005; Tyson and Preston-Whyte 2000). Harrison (1984) reported in his study that tropical and temperate perturbations are major determinants of southern African rainfall. Deep tropical lows and deep temperate lows are low level circulation centres in the Rossby waves. The deep tropical and temperate low can intensify into a cyclone and if more intense, can lead to a

storm. Tropical easterly lows are caused by disturbances in the easterly wave, driven largely by thermal heating of the continent. They help in tropical moisture and energy transfer. This process significantly facilitates rainfall over the region (Mason and Jury 1997; Van den Heever et al. 1997). Also, Miron and Tyson (1984) found that synoptic situations responsible for rain-bearing winds are consistent with easterly low disturbances. The tropical and temperate easterly lows are responsible for rainfall over the interior during summer.

The transient circulation features occur progressively as they change from one form to the other on a day-to-day basis. In one case, troughs and ridges occur and eventually develop into cut-off lows (Hobbs et al. 1998; Tyson and Preston-Whyte 2000; Browning and Mason 1980; Fuenzalida et al 2005; Smith and Reeder 1988; Garreaud 2000). In another case, when the upper westerly wave coincides with an easterly wave or depression in lower levels, it results in the formation of a tropical temperate trough. This feature is associated with tropical moisture and energy transfer and it has been known to significantly contribute to summer rainfall over southern Africa (Harangozo and Harrison 1983; Harrison 1984b).

This study reports the capability of CAM3 and HadAM3 in simulating the mean number of cut-off lows, number of days with tropical lows, temperate lows and tropical temperate troughs (TTTs) from 1971 through 2000. In addition, we report how the small scale features are related to the rainfall variability over southern Africa.

2. Model Description and Techniques

HadAM3 is the atmosphere component of the Hadley Centre Coupled Model version 3 (HadCM3) (Gordon et al. 2000; Pope et al. 2000), which was developed at the Hadley Centre for Climate Prediction and Research, UK. HadAM3 has been used for operational seasonal forecast over South Africa by the Climate Systems Analysis Group, University of Cape Town since 1971. In this study, the horizontal resolution of HadAM3 used is 3.75^{o} longitude, 2.5^{o} latitude, and 8 layers in the vertical which are based on a hybrid vertical coordinate system (Simmons and Burridge 1981). The model employs spherical polar coordinates on a regular latitude-longitude grid. The development and description of the HadAM3 model can be found in Gordon et al. 2000; Pope et al. 2000; Jones et al. 2005; Murphy et al. 2002. The work of Hudson and Jones (2002) concluded that the model is generally able to capture the circulation dynamics of the present-day climate.

The CAM3 model is the atmosphere component of Community Climate System Model, version 3.0 (CCSM3) (Collins et al. 2004), which was developed at the US National Centre for Atmospheric Research (NCAR). In this study, the finite volume dynamic core

option, with horizontal resolution of 2.0^o x 2.5^o and 26 vertical levels were used.

Both HadAM3 and CAM3 were applied to produce 30 years (1971-2000) climate simulation with 5 member ensembles of daily data each. Statistical average of these ensemble members' estimation of the features were used in the analysis. In the simulation, the observed SST as the lower boundary forcing was used. For better comparison, the models results were interpolated to the resolution (2.5^o x 2.5^o) of the NCAR reanalysis I data (NCEP). ERA40 reanalysis rainfall and temperature were used.

In the investigation of the models to reproduce the small scale features, the simulated 500hPa and 850hPa geopotential heights simulations were analyzed and the results compared with those from NCEP reanalysis. The standardized anomalies calculated from the mean of daily geopotential height from a time series of 1971 through 2000 period were done to take care of the seasonal variations within the dataset. This removes dispersion in the dataset and helps to recognize the magnitude of the anomalies. Additionally, we use the Laplace equation to track cut-off lows, temperate and tropical lows. The tropical temperate trough is defined as a tropical low coupled to a cut-off low through a subtropical trough (Mason and Jury 1997). The tropical region is defined in this study as 25^{o}S – 0 and 0 – 50^{o}E and the temperate region as 50^{o}S – 25^{o}S and 0 – 50^{o}E. The identification of depressions was based on an 8 neighbour grid value of a two dimensional geopotential field at 500hPa for cut-off lows and tropical temperate troughs; 500hPa and 800hPa for deep tropical and temperate lows.

3. Results

a. Mean Climatologies

The mean rainfall over southern Africa from 1971 through 2000 from ERA0 reanalysis, CAM3 and HadAM3 is shown in Figure 1. The mean rainfall increases towards the equator from the south of the region. A minimum of 1mm/day is observed over the ocean and a maximum of 6mm/day near the equator in ERA40. Dryness to very low rainfall emerges from the Atlantic Ocean into the continent over most of the western and central part of the region. About 3mm/day rainfall is observed over a small region at the Eastern Cape in South Africa. Few differences can be seen in the models reproducing the mean rainfall. Particularly in CAM3, the dryness that emerges from the Atlantic Ocean is only over Cape Town. The prominent features to note here are the two maximum regions (instead of one) simulated by CAM3 near the equator between 25^{o}E and 30^{o}E and also between 40^{o}E and 50^{o}E. The peak near the equator, between 40^{o}E and 50^{o}E, decreases south eastwards in the Indian Ocean between Madagascar and southern Africa. Again, the model simulates a small region of low

rainfall over the eastern part of the southern continent, which is not seen in ERA40. HadAM3 generally underestimates the mean rainfall over southern Africa. However, the pattern of the mean is fairly close to the pattern seen in ERA40. It is able to capture the 3mm/day rainfall over the small region at the Eastern Cape in South Africa as seen in the ERA40.

In figure 2, the mean of the temperature from 1971 through 2000 is shown from ERA40 reanalysis, CAM3, and HadAM3. The minimum temperature seen in ERA40 is 14^{o}C over the Atlantic Ocean and it increases into the continent. Another minimum is located over a small region at the Eastern Cape in South Africa. Two maximum regions are found in the pattern; between 25^{o}S and the equator in the western and eastern parts of the domain. The models simulate a similar pattern but generally underestimate the mean temperature in most parts of the region. HadAM3 particularly captures the minimum over a small region at the Eastern Cape in South Africa as seen in ERA40.

Figure 3 shows the mean geopotential height at 500hPa pressure level from NCEP reanalysis, CAM3, and HadAM3 models. The mean height is calculated from 30 years simulation from the models and is shown in meters with an interval of 40m. The mean height is observed in NCEP to increase from south to north of the region. This field is about 5650m over the southern Oceans, it increases vertically towards the equator to a high mean height of 5860m near the equator. The models reproduce similar patterns of this mean geopotential height. Particularly, HadAM3 reproduces almost the same as that observed from NCEP reanalysis. In CAM3, the maximum of the mean height is concentrated in the central part of the region; it does not reach the equator, as observed in the NCEP. Near the equator at the west and some parts of the eastern region, a height of about 5800m is simulated by CAM3.

b. Seasonal Variations

The seasonal variations in the simulated climatological rainfall from the models and ERA40 are shown in figure 4a. The models show a good agreement with ERA40 reanalysis but CAM3 over predicts the summer rainfall (by about 2 mm/day) while HadAM3 under predicts it by about 1 mm/day. Similarly, in figure 4b the maximum climatological temperature is in summer and the minimum temperature is in winter. CAM3 over predicts March, April and May temperatures by 1^{o}C and HadAM3 under predicts the JJA temperatures by 1^{o}C.

The seasonal variation of the standardized rainfall and temperature anomalies over southern Africa for the 1971-2000 year period are shown in figure 5. The standardized anomalies are calculated from their daily anomalies and climatological standard deviations. In figure 5a, positive standardized anomaly of rainfall almost equal to 1 is observed, from NCEP,

in January and it decreases to zero at the end of April. The negative anomaly starts in May and peaks in July, it then rises through to October. Positive anomaly starts again at the beginning of November and it increases in December. The models simulate these anomalies precisely. Both have a correlation coefficient of 0.98 with ERA40 reanalysis. In figure 5b, positive standardized anomaly of temperature decreases from 1 in January to zero at the end of April. The negative anomaly starts in May at zero and decreases to near -1.5 in mid July, it then increases gently from -1.5 in July to zero in October. The Positive anomaly starts again in October at zero to a little above 0.5 in December. The models are estimating standardized anomaly.

Figure 6 compares the models standardized anomalies of their daily geopotential height at 500hPa pressure level (figure 6a) and near the surface at 850hPa pressure level (figure 6b) with NCEP reanalysis. In figure 6a, NCEP shows a positive anomaly that increases from January till May and in December. The positive anomaly peaks in March at 1.5 and decreases to zero in May. The negative anomaly is between 0 and -1.5, within this range, the standardized anomaly decreases from zero in May to -1.5 in August but rises again between August and November. Similarly, both models simulate a similar pattern in the range of their deviations. In particular, CAM3 reproduces the positive anomalies from January through May and negative anomalies between June and November. December has positive anomalies. The peak of the positive anomalies in this case is in April. Like in NCEP, CAM3 simulates the negative anomalies from June through November. Moreover, CAM3 shows a correlation coefficient of 0.89 with the NCEP. Interestingly, HadAM3 reproduces very a similar pattern as in NCEP with a correlation coefficient of 0.94. In figure 6b, negative anomalies at 850hPa are observed from January through May and from October through December. The winter months starting from May have positive anomalies up to about 1.5. The range is between -1.5 and 1.5. The models simulate the range of the standardized deviation as in NCEP. However, CAM3 simulates the transition from negative to positive anomaly more than a month earlier, sometime in March while HadAM3 has a closer transition time as NCEP.

Figure 7 shows the seasonal mean number of cut-off lows estimated from NCEP and the models. A high mean number of cut-off lows is observed from NCEP during the onset of the austral winter season in March and April from NCEP. A smaller peak is present in October. Both models capture the peak of the mean number of cut-off lows in March but they represent the second peak (in October for NCEP) a bit earlier in September. Although, both models generally under estimate the mean number of cut-off lows over the region, HadAM3 simulates the mean number closer to that of NCEP reanalysis with a correlation coefficient of

0.63 with NCEP.

In figure 8a, the observed number of days with deep tropical lows from NCEP varies between 17 and 30 per month. The highest number of days with tropical lows from NCEP is close to 30 in February. The number of days with deep tropical lows decreases as winter approaches. May, June and July recorded the lowest number of days with tropical lows and 17 days is the observed minimum. The number of days increases from July through December and from January through February. Both models underestimate the number of days with deep tropical lows although they show similar pattern to that of NCEP. For CAM3, the months January, February, March and December have 25 days of deep tropical lows. The number of days with tropical lows decreases to 15 in April and May then increases from 15 to 20 through June. CAM3 has a correlation coefficient of 0.87 with NCEP. In the case of HadAM3, the number of days with deep tropical lows is in the order of 5 to 20 days from January through December. It also reproduces less number of days with tropical lows from the onset of winter season in May till the peak of winter season in July but the correlation coefficient is still high (0.83).

In addition, the number of days with deep temperate lows from NCEP reanalysis and the models is shown in figure 8b. Generally, lower number of days with deep lows is seen from NCEP over the temperate region than over the tropical region (see figure 8a). The number of days with deep temperate lows increases from September through December and also from January through March. The highest number of days with deep temperate lows from NCEP in March is 8. The NCEP reanalysis shows the lowest number of days with deep temperate lows to be 4 per month during the austral winter season. The models extremely underestimate the number of days with deep temperate lows. CAM3 particularly estimates almost zero number of days per month of temperate lows in winter and close to 1 day per month in summer. HadAM3 estimates about 2 days of temperate lows in summer and winter months have between zero and 1 day of temperate lows per month. The highest estimated number of days of these lows is close to 3 in April. The models have a correlation coefficient of 0.59 and 0.47 for CAM3 and HadAM3, respectively.

Figure 9 shows the seasonal variation of days with TTTs from 1971 to 2000 over the same domain. It is evident that the number of days with TTTs estimated from NCEP increases from September through March. The number of days with TTTs from NCEP is between 4 and 8 throughout the seasons. The pattern is reproduced fairly in both models except with CAM3, which overestimates the number of days with TTTs throughout the year and more significantly in January, February, March and December. HadAM3 reproduced the number of

days with TTTs between 4 and 8, as seen from NCEP reanalysis.

4. Discussion

Most of the synoptic scale features presented here are rainfall inducing systems, which are noticeable at the 500hPa pressure level. As seen in the spatial patterns, the mean geopotential height at 500hPa pressure level is similar to that of the mean rainfall and temperature over the study region. Negative anomalies in the daily geopotential height at 500hPa correspond to low climatological rainfall between May and November. In contrast, at the 850hPa (figure 5b), positive anomalies in the daily geopotential height correspond to low climatological rainfall between May and October. The link between the 850hPa geopotential height and rainfall has been reported in a related study by Landman and Goddard (2002) using a pattern analysis from Canonical Correlation Analysis.

Moreover, from figures 7 and 4a, as the mean number of cut-off lows increases, there is an increase in the mean rainfall and when the mean number of cut-off lows decreases, the mean rainfall decreases. However, a correlation coefficient of 0.44 not significant at 95% confidence level is shown for cut-off lows from NCEP and ERA40 rainfall (table 1). CAM3 also shows a low correlation coefficient for cut-off lows and rainfall, which is not significant. In table 1, HadAM3 shows a high correlation coefficient for cut-off lows and rainfall which is significant at 95% level of confidence.

In addition, the months with a high number of days of TTTs correspond to months with high rainfall. The link between TTTs and rainfall over southern Africa has been explained through moisture convergence by Todd and Washington (1999). Also, low number of days of temperate lows agrees with low winter rainfall over southern Africa. It can be seen in table 1, that there is a significant correlation coefficient from NCEP for tropical lows, temperate lows, TTTs and ERA40 rainfall at 95% confidence level. Similarly, CAM3 also shows high correlation coefficients which are significant at the same confidence level for the same features and rainfall. However, HadAM3 shows a strong correlation coefficient for tropical lows and for TTTs but no relationship at all for temperate lows. The pattern of the features discussed above can be confirmed from related studies (Harrison 1984a; Miron and Tyson 1984; Tyson 1986; Mason and Joubert 1997; Todd and Washington 1999).

5. Conclusion

The models have shown their capabilities in reproducing the small scale features over southern Africa in comparison with the NCEP reanalysis. The variations in the geopotential

height has been studied with the models and compared with NCEP reanalysis. The variability of the small scale features is associated with the position and intensity of rainfall over the region. The models correlate well with NCEP in the standardized geopotential height anomalies at both 500hPa and 850hPa pressure levels. The variations in the geopotential height have been linked with rainfall and temperature through their means and standardized anomalies. The standardized anomalies in the geopotential height at 500hPa pressure level have been shown to be in phase with the standardized anomalies of rainfall and that at 850hPa pressure level to be out of phase with that of rainfall and temperature. In the summer months (DJF), when the region experiences maximum rainfall, small scale features like cut-off lows, tropical lows and TTTs show increased intensity. Also during winter, low rainfall corresponds to low intensity of the small scale features. The seasonal variation in tropical lows, temperate lows and TTTs has also been shown to relate with the mean rainfall with strong correlation coefficient, which are significant at 95% confidence level.

Generally, the models are able to reproduce the synoptic scale circulation features and have estimated the relationship between them and rainfall. These features are crucial for reliable seasonal forecast over southern Africa. Moreover, the accuracy of forecast produced from these global models will depend on the ability of these GCMs to simulate the synoptic scale circulation features that play dominant roles in determining the climate over the region.

Acknowledgments

The project is sponsored by Centre for High Performance Computation (CHPC South Africa) and Department of Energy (DOE, USA). The first author is grateful to Schlumberger and DAAD for financial support. The second author is grateful to John Standford for financial support under the incentive project funds at Iowa State University. The authors appreciate the technical support of Climate Systems Analysis Group staff. This work was done within the framework of the Associateship Scheme of the Abdus Salam International Centre for Theoretical Physics, Trieste, Italy.

References

Anyah RO, Semazzi FHM (2006) NCAR-AGCM ensemble simulations of the variability of the Greater Horn of Africa climate, Special Issue, Theoretical and Applied Climatology, 86, 39-62.

Browning K, Mason J (1980) Air motion and precipitation growth in frontal systems. Pure and Applied Geophysics, 119 (3) : 577–593.

Collins WD, Rasch PJ, Boville BA, Hack JJ, McCaa JR, Williamson DL, Kiehl JT, Briegleb B (2004) Description of the NCAR Community Atmosphere Model (CAM 3.0), NCAR Technical Note, pp. 1-226.

Fuenzalida H, Śnchez R, Garreaud R (2005) A climatology of cutoff lows in the Southern Hemisphere. J. Geophys. Res, 110.

Garreaud R (2000) Cold Air Incursions over Subtropical South America: Mean Structure and Dynamics. Monthly Weather Review, 128(7):2544–2559.

Gordon C, Cooper C, Senior C, Banks H, Gregory J, Johns T, Mitchell J, Wood R (2000) The simulation of SST, sea ice extents and ocean heat transports in a version of the Hadley Center coupled model without flux adjustments. Climate Dynamics, 16(2):147–168.

Harangozo A, Harrison MSJ (1983) On the use of synoptic data in indicating the presence of cloud bands over southern Africa. South African J. Sci. 70, 413–414.

Harrison, M (1984a) A generalized classification of South African summer rain-bearing synoptic systems. International Journal of Climatology, 4(5).

Harrison M (1984b) The annual rainfall cycle over the central interior of South Africa. S. Afr. Geogr. J, 66:47–64.

Hudson D, Jones R (2002) Simulations of present-day and future climate over southern Africa using HadAM3H. Hadley Center Technical Note, 38.

Hobbs JE, Lindsay JA, Bridgman HA (1998) Present Climates of Australia and New Zealand. Climates of the southern continents: present, past, and future, John Wiley & Sons Chichester, United Kingdom. pp 63-105.

Jones C, Gregory J, Thorpe R, Cox P, Murphy J, Sexton D, Valdes P (2005) Systematic optimisation and climate simulation of FAMOUS, a fast version of HadCM3. Climate Dynamics, 25(2):189–204.

Jury MR, Nkosi SE (2000) Easterly flow in the tropical Indian Ocean and climate variability over south-east Africa, Water SA, 26, 147-152.

Landman WA, Goddard L (2002) Statistical Recalibration of GCM Forecasts over Southern Africa Using Model Output Statistics. J. Climate, 15, 2038–2055.

Mason SJ, Joubert AM (1997) Simulated changes in extreme rainfall over southern Africa. Int. J. Climatol., 17, 291–301.

Mason S, Jury M (1997) Climatic change and inter-annual variability over southern Africa: a reflection on underlying processes. Progress in Physical Geography, 21:24–50.

Miron O, Tyson P (1984) Wet and Dry Conditions and Pressure Anomaly Fields over South Africa and the Adjacent Oceans, 1963–79. Monthly Weather Review, 112(10):2127–2132.

Murphy B, Marsiat I, Valdes P (2002) Atmospheric contributions to the surface mass balance of Greenland in the HadAM3 atmospheric model. Journal of Geophysical Research (Atmospheres), 107(D21).

Nieto R, Gimeno L, d la Torre L, Ribera P, Gallego D, Garcı́-Herrera R, Garcıa´ JA, Nunez M, Redano A, Lorente J (2005) Climatological features of cut-off low systems in the northern hemisphere. J Climate, 108:3085–3103. doi: 10.1175/JCLI3386.1

Pope V, Gallani M, Rowntree P, Stratton R (2000) The impact of new physical parametrizations in the Hadley Centre climate model: HadAM3. Climate Dynamics, 16(2):123–146.

Qiu B, Chen S, Hacker P (2004) Synoptic-Scale Air–Sea Flux Forcing in the Western North Pacific: Observations and Their Impact on SST and the Mixed Layer. J. Phys. Oceanogr., 34: 2148–2159.

Reason CJC, Jagadheesha D (2005) A model investigation of recent ENSO impacts over southern Africa. Meteorology and Atmospheric Physics, Special Issue on Regional Climate Change and Variability, 89(1):181–205. DOI 10.1007/s00703-005-0128-9.

Simmons A, Burridge D (1981) An Energy and Angular-Momentum Conserving Vertical Finite-Difference Scheme and Hybrid Vertical Coordinates. Monthly Weather Review, 109(4):758–766.

Smith R, Reeder M (1988) On the Movement and Low-Level Structure of Cold Fronts. Monthly Weather Review, 116(10):1927–1944.

Taljaard J, Bureau W (1985) Cut-off lows in the Southern African region. South African Weather Bureau Technical Paper No.14.

Todd MC, Washington R (1999) Circulation anomalies associated with Tropical-Temperate Troughs in Southern Africa and the South West Indian Ocean. Climate Dynamics, 15, 937-951.

Tyson PD (1981) Atmospheric circulation variations and the occurrence of extended wet and dry spells over Southern Africa. J Climatol 1:115–130.

Tyson PD (1986) Climate Change and Variability in Southern Africa. Cape Town: Oxford Univ. Press, 220 pp.

Tyson P, Preston-Whyte R (2000) The Weather and Climate of Southern Africa. Oxford University Press.

Van den Heever S, D'Abreton P, Tyson P (1997) Numerical simulation of tropical-temperate troughs over southern Africa using the CSU RAMS model.

Table 1. Correlation coefficients between Small scale features and rainfall from NCEP, CAM3 and HadAM3. Values with * are not significant at 95% confidence level

	Cut-off lows	Tropical lows	Temperate lows	Tropical Temperate Troughs
NCEP	0.44*	0.84	0.89	0.88
CAM3	0.39*	0.95	0.78	0.85
HadAM3	0.83	0.89	0.00*	0.72

Figures captions

Fig 1. Rainfall mean (mm/day) for 30yrs from ERA40 (upper row), CAM3 (middle row) and HadAM3 (bottom row)

Fig 2. Temperature mean (^{o}C) for 30yrs from ERA40 (upper row), CAM3 (middle row) and HadAM3 (bottom row)

Fig 3. Mean of geopotential height (m) at 500hPa level from NCEP (upper row), CAM3 (middle row) and HadAM3 (bottom row)

Fig 4. Seasonal variation in climatological rainfall (a) and temperature (b) over southern Africa (0-50E, 40S-0) from ERA40 (deep solid), CAM3 (dashed) and HadAM3 (light solid)

Fig 5. Standardized anomalies of rainfall (a) and temperature (b) over southern Africa (0-50E, 40S-0) from ERA40 (deep solid), CAM3 (dashed) and HadAM3 (light solid)

Fig 6. Standardized anomalies of geopotential height at 500hPa (a) and at 850hPa (b) over southern Africa (0-50E, 40S-0) from NCEP (black), CAM3 (deep grey) and HadAM3 (light grey)

Fig 7. Seasonal variation of mean number of cut-off lows over southern Africa (0-50E, 40S-0) from NCEP (deep solid), CAM3 (dashed) and HadAM3 (light solid)

Fig 8. Seasonal variation of number of days with tropical lows (a) and temperate lows (b) over southern Africa (0-50E, 40S-0)

Fig 9. Seasonal variation of number of days with tropical temperate troughs over southern Africa (0-50E, 40S-0)

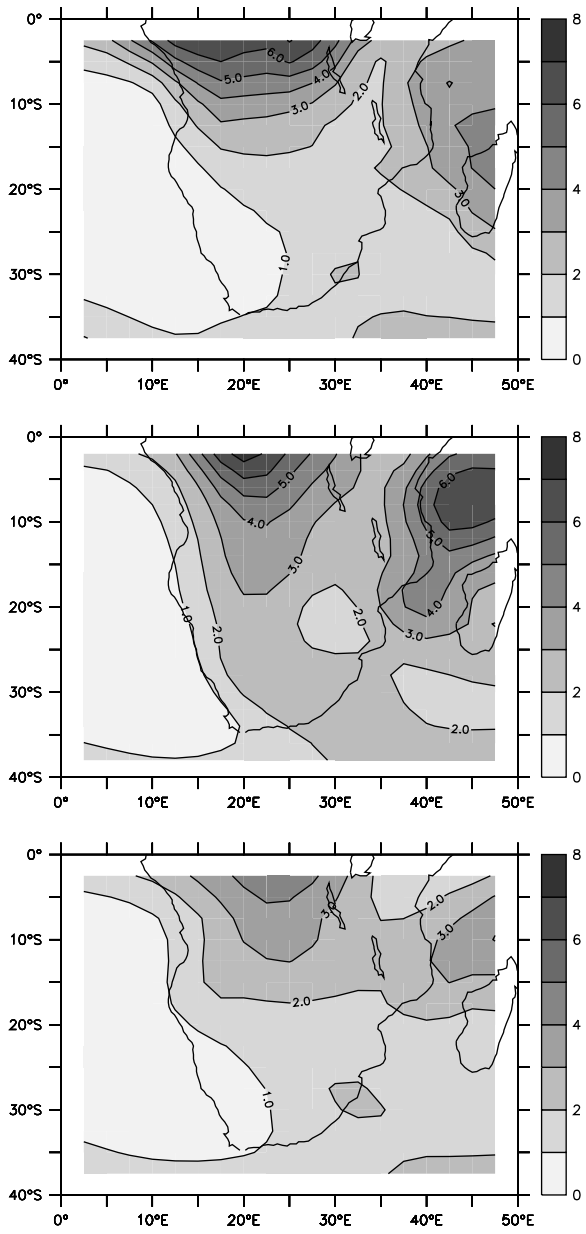

Fig.1

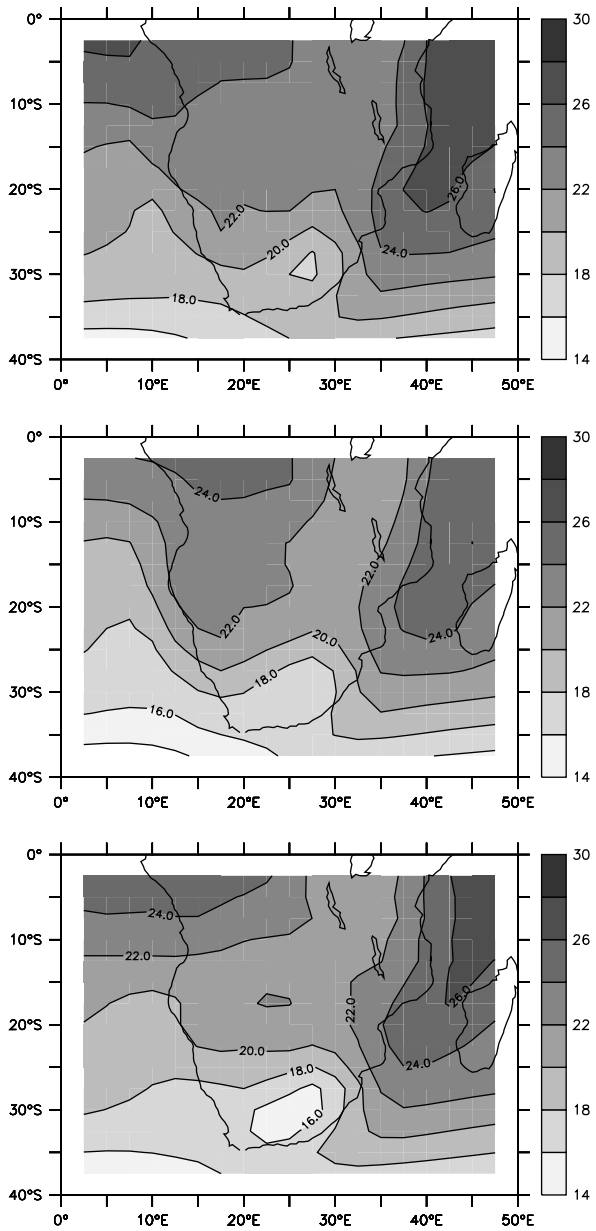
0°
10°S
20°S
30°S
40°S
0°
10°E
20°E
30°E
40°E
50°E
30
26
22
18
14
26.0
22.0
20.0
24.0
18.0
24.0
22.0
22.0
20.0
18.0
16.0
24.0
22.0
22.0
26.0
20.0
18.0
24.0
16.0

Fig.2

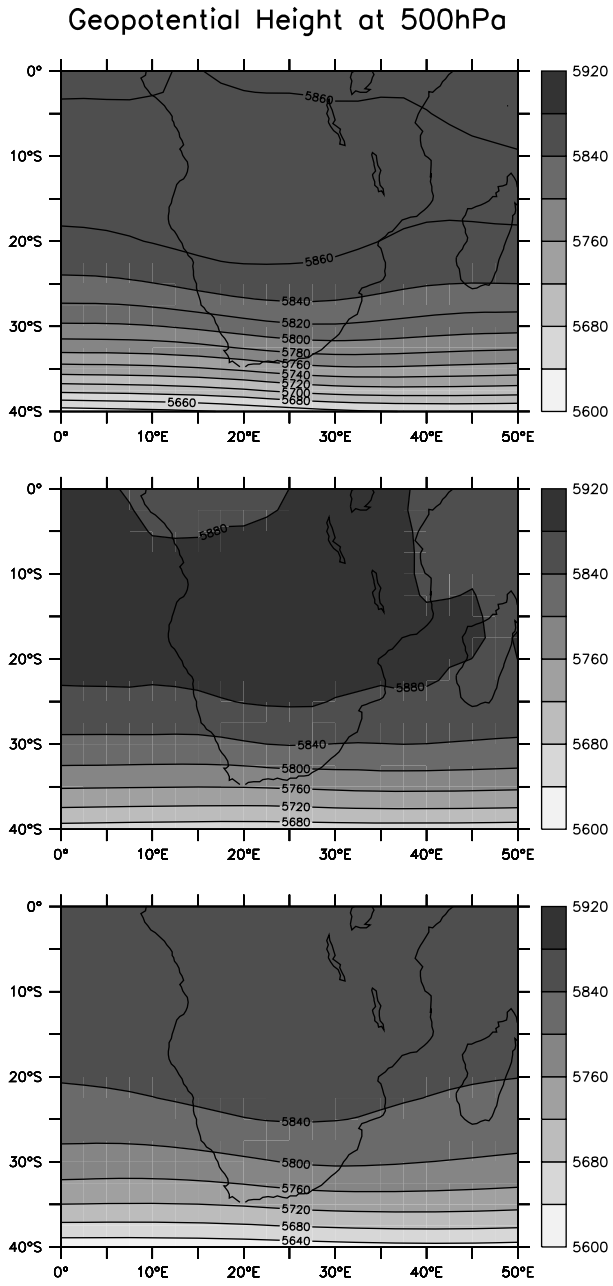
Geopotential Height at 500hPa
0°
10°S
20°S
30°S
40°S
0°
10°E
20°E
30°E
40°E
50°E
5920
5840
5760
5680
5600
5860
5840
5820
5800
5780
5760
5740
5720
5700
5680
5660
5880
5840
5800
5760
5720
5680
5840
5800
5760
5720
5680
5640

Fig.3

(a)

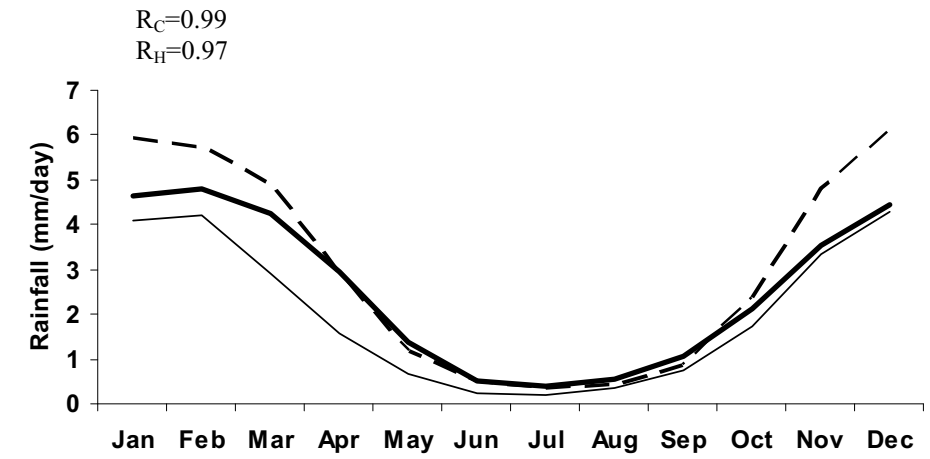
R_C=0.99
R_H=0.97
Rainfall (mm/day)
0
1
2
3
4
5
6
7
Jan
Feb
Mar
Apr
May
Jun
Jul
Aug
Sep
Oct
Nov
Dec

(b)

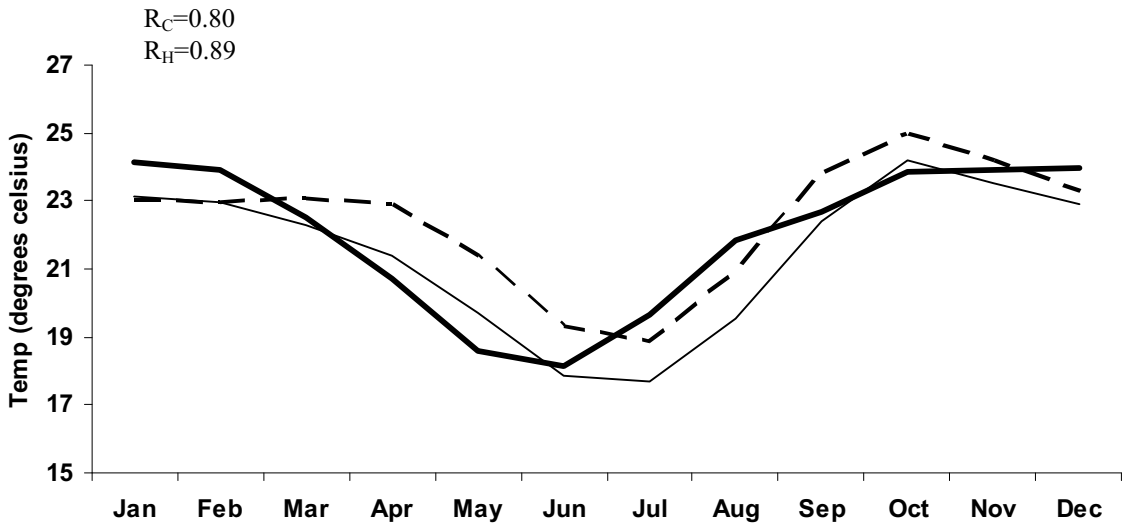
R_C=0.80
R_H=0.89
Temp (degrees celsius)
15
17
19
21
23
25
27
Jan
Feb
Mar
Apr
May
Jun
Jul
Aug
Sep
Oct
Nov
Dec

Fig. 4

(a)

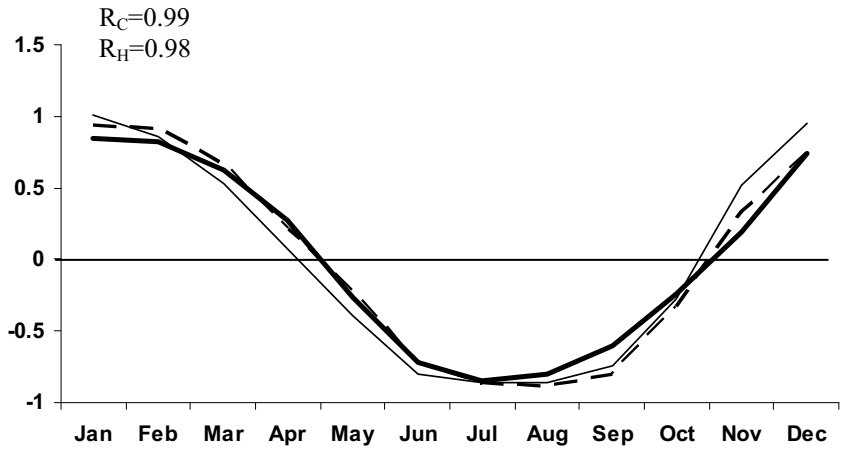
R_C=0.99
R_H=0.98
1.5
1
0.5
0
-0.5
-1
Jan
Feb
Mar
Apr
May
Jun
Jul
Aug
Sep
Oct
Nov
Dec

(b)

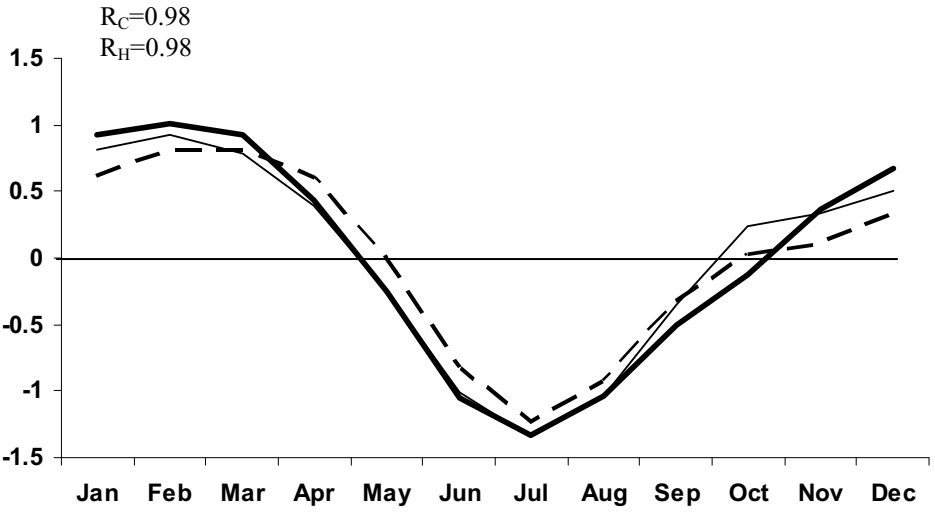
R_C=0.98
R_H=0.98
1.5
1
0.5
0
-0.5
-1
-1.5
Jan
Feb
Mar
Apr
May
Jun
Jul
Aug
Sep
Oct
Nov
Dec

Fig. 5

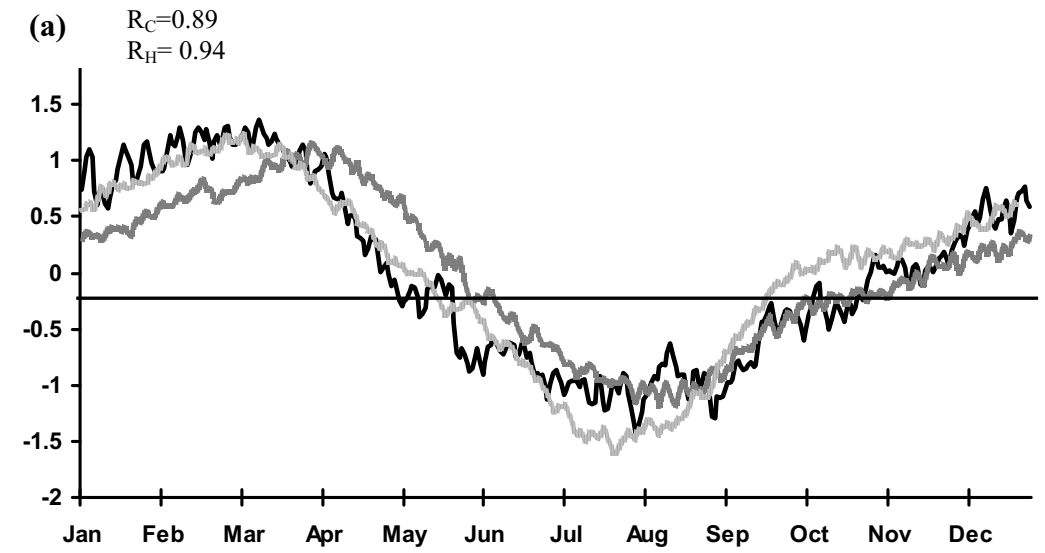
(a)
R_C=0.89
R_H= 0.94
1.5
1
0.5
0
-0.5
-1
-1.5
-2
Jan
Feb
Mar
Apr
May
Jun
Jul
Aug
Sep
Oct
Nov
Dec

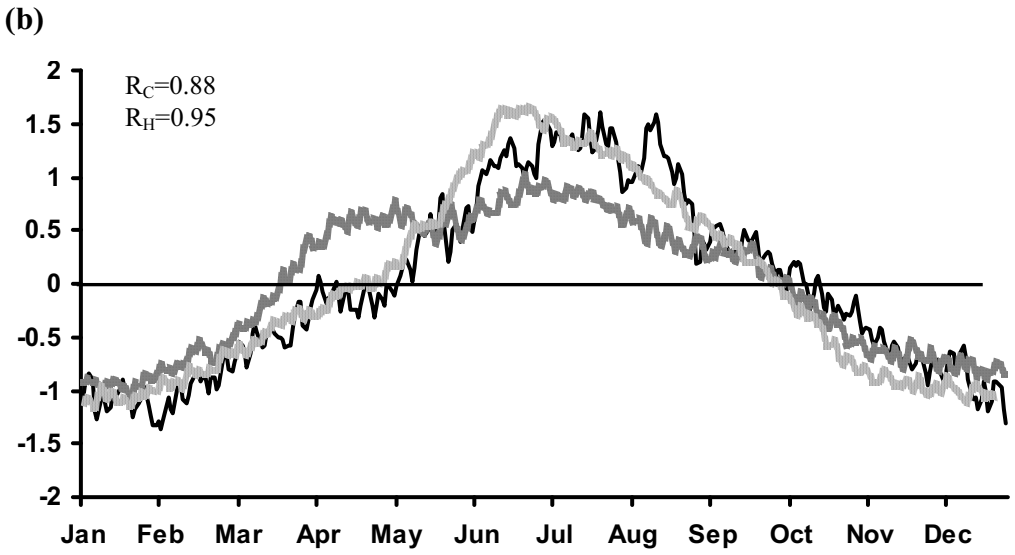
(b)
R_C=0.88
R_H=0.95
2
1.5
1
0.5
0
-0.5
-1
-1.5
-2
Jan
Feb
Mar
Apr
May
Jun
Jul
Aug
Sep
Oct
Nov
Dec

Fig. 6

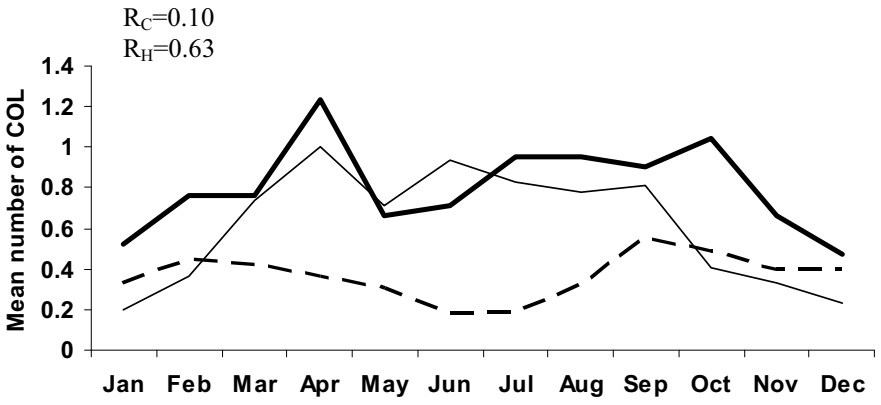
R_C=0.10
R_H=0.63
Mean number of COL
1.4
1.2
1
0.8
0.6
0.4
0.2
0
Jan
Feb
Mar
Apr
May
Jun
Jul
Aug
Sep
Oct
Nov
Dec

Fig. 7

(a)

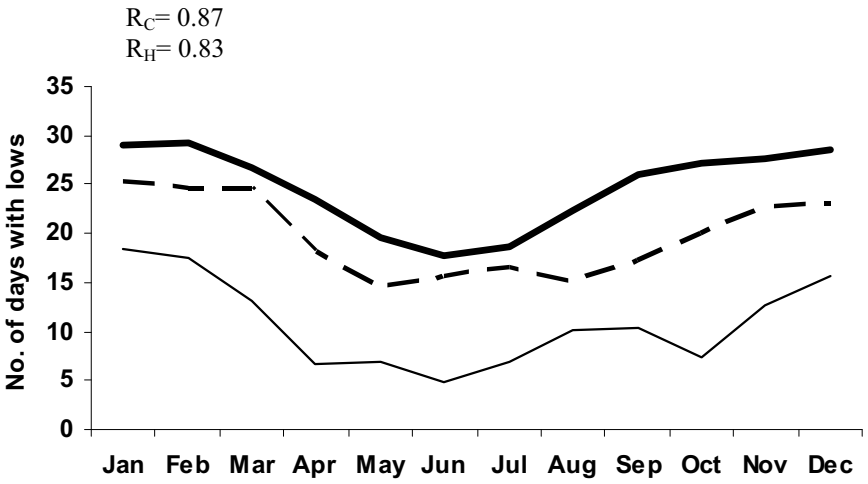
R_C= 0.87
R_H= 0.83
No. of days with lows
35
30
25
20
15
10
5
0
Jan Feb Mar Apr May Jun Jul Aug Sep Oct Nov Dec

(b)

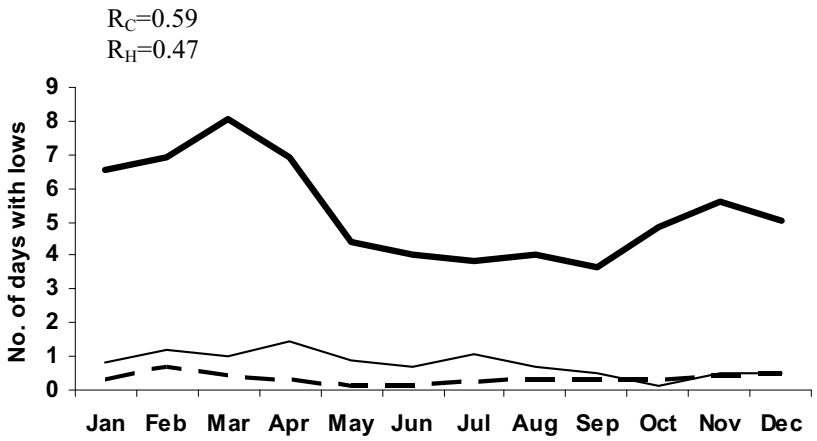
R_C=0.59
R_H=0.47
No. of days with lows
9
8
7
6
5
4
3
2
1
0
Jan Feb Mar Apr May Jun Jul Aug Sep Oct Nov Dec

Fig. 8

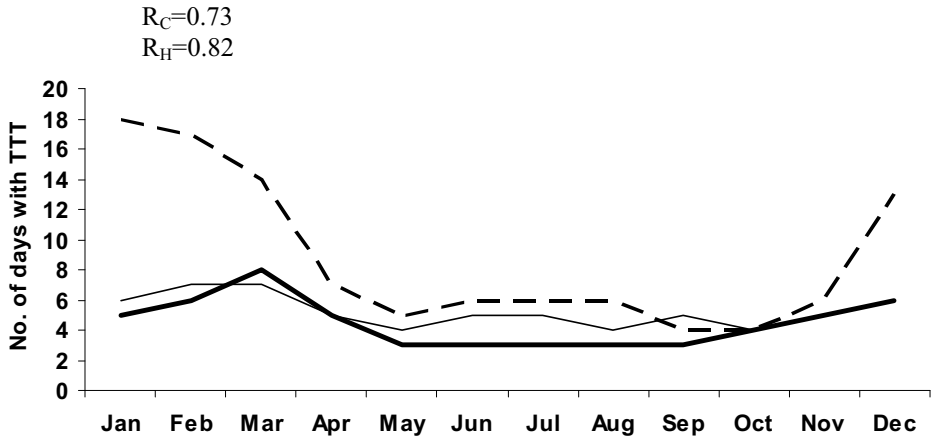
R_C=0.73
R_H=0.82
No. of days with TTT
20
18
16
14
12
10
8
6
4
2
0
Jan
Feb
Mar
Apr
May
Jun
Jul
Aug
Sep
Oct
Nov
Dec

Fig. 9